INTEGRATING THERMAL CONSTRAINTS INTO HABITAT SUITABILITY FOR MOOSE IN THE ADIRONDACK STATE PARK, NEW YORK

Catherine G. Haase[1] and H. Brian Underwood[2]

[1]State University of New York College of Environmental Science and Forestry, Department of Environmental and Forest Biology, 212 Illick Hall, 1 Forestry Drive, Syracuse, New York 13210; [2]USGS Patuxent Wildlife Research Center, State University of New York College of Environmental Science and Forestry, Department of Environmental and Forest Biology, 426 Illick Hall, 1 Forestry Drive, Syracuse, New York 13210, USA.

ABSTRACT: Moose (*Alces alces*) survive cold winter temperatures due to their large body size, thick skin, and dense, dark pelage. These same characteristics impede heat dissipation under thermal conditions often encountered in spring-fall. While thermal cover has long been recognized as an important component of moose habitat suitability, it has not been explicitly incorporated into published models. We integrated the biophysical construct of operative temperature, T_e, into an existing Habitat Suitability Index (HSI) model for moose in the Adirondack State Park (ASP) of New York. T_e is a thermal index that incorporates the effects of radiative and convective heat transfer on air temperature. We modeled air temperature with respect to elevation and calculated solar radiation transmitted through the canopy as a function of topography, location, forest cover-type, and time of year. We classified 1028, 25 km^2 evaluation units for thermal suitability based on a modified upper critical threshold for T_e derived from published studies. Compared to a published model for ASP, our HSI better classified moose observations in low, moderate, and high suitability categories, especially during April. We discuss the complexities of modeling thermal suitability for moose.

ALCES VOL. 49: 49–64 (2013)

Key words: Adirondacks, *Alces alces*, habitat suitability, heat stress, moose, operative temperature, thermal cover.

Wildlife biologists and forest managers focus on the relationship between an animal species and its preferred habitat for developing appropriate management practices (Guisan and Zimmerman 2000). This relationship is important to evaluate an area relative to the animal's survival and reproduction (Puttock et al. 1995). There are various tools for habitat analyses, including resource selection functions, occupancy models, and habitat suitability index (HSI) models. HSI models are graphical constructs that quantify habitat quality in response to food and cover requirements of a species (Koitzsch 2002). These models rate suitability on a scale of 0.0 (unsuitable habitat) to 1.0 (optimal habitat) with different compartments or areas scored in relation to life requisites (Romito et al. 1999), and allow for comparisons among managed areas as well as focusing on increasing suitability scores by managing for resources that are limiting (Koitzsch 2002, Dussault et al. 2006). It is assumed that a species will be present and more abundant in areas with higher suitability; wildlife managers can therefore validate HSI models by measuring habitat characteristics and correlating the calculated scores with population data (Dettki et al. 2003, Dussault et al. 2006).

HSI models have been used in moose (*Alces alces*) management since the U.S. Fish and Wildlife Service (USFWS) first published procedures in the early 1980s when Allen et al.

(1987) described the first 2 USFWS models: Model I required detailed vegetation measurements and habitat assessment, whereas Model II focused on remotely-sensed data in its classification of suitable habitat. Remote sensing has allowed both models to be applied to large tracts of land without the time and spatial constraints of field-based methods (Koitzsch 2002, Hickey 2008). Although originally created for the Lake Superior region, Model II was used with remotely-sensed data in Geographic Information System (GIS) to assess habitat suitability relative to regenerating forests and non-forested wetlands in Vermont (Koitzsch (2002). Hickey (2008) used a similar approach and speculated about future growth of the recolonizing moose population in the Adirondack State Park (ASP) in New York.

In addition to requiring large tracts of land with diverse vegetation types (Dussault et al. 2006), moose require 40–50% of an area to be comprised of suitable habitat with regenerating woody stems essential for late-summer and winter forage, 5–10% in non-forested, macrophyte-rich wetlands necessary for summer forage, and 5–55% comprising dense forest stands critical for thermal cover in late winter and summer months (Renecker and Hudson 1986, Schwab and Pitt 1991, Puttock et al. 1995, Koitzsch 2002). While the GIS-based models of Koitzsch (2002) and Hickey (2008) acknowledged the importance of these criteria, neither measured nor included thermal cover explicitly.

Renecker and Hudson (1986) first noted that although moose are adapted to live in cold environments, they exhibit heat stress at temperatures as low as −5 °C in the late winter and 14 °C in the summer. Chronic heat stress may lead to increased susceptibility to parasitism and disease, reduced productivity, and starvation (Renecker and Hudson 1990, Lenarz et al. 2008). Moose respond behaviorally to heat stress by seeking cover under dense coniferous forest canopies, by prostrating themselves on cool substrates (e.g., soil or snow), by immersing themselves in water (Dussault et al. 2004), and by reducing voluntary food intake (Belovsky 1981). The gradual 40-year decline in moose populations in Isle Royale National Park in Michigan and in the Agassiz National Wildlife Refuge in northern Minnesota are correlated with increasing temperatures associated with climate change, and speculation exists about the role of increased parasitism and heat stress (Murray et al. 2006, Lenarz et al. 2008). Projections of climate-warming scenarios indicate a future ASP forest with fewer coniferous trees, warmer and shorter winters with decreased snowpack and longer ice-free periods, and hotter, longer summers (Jenkins 2004).

We attempted to incorporate an index of thermal suitability into a Model II approach for assessing moose habitat in the ASP. We evaluated critical thermal environments (Moen 1968, Parker and Gillingham 1990) for moose by computing operative temperature (T_e), an index that integrates the combined effects of ambient temperature, total absorbed radiation, and wind velocity on the thermal environment experienced by an animal (Bakken 1992). T_e considers the effects of pelage on heat loss and heat absorption and incorporates seasonal variation in surface albedo due to accumulated snow. Air temperature was incremented above ambience to indicate the temperature of a space that would feel the same as the heat load in the sun (Campbell and Norman 1997).

Integrating thermal cover as a habitat variable not only allows assessment of current suitability, but also facilitates prediction of future suitability under climate-warming scenarios (Koitzsch 2002). By mapping T_e across the ASP, our goal was to stimulate discussion and additional research regarding critical thermal environments as components

of habitat suitability for moose. Our specific objectives were to 1) develop an HSI model for moose that incorporates thermal suitability in a spatially explicit manner, and 2) compare the HSI performance against a published model (Hickey 2008) lacking a specific thermal component.

STUDY AREA

The ASP is located in the northeastern part of New York State (latitude 44E 00" N, longitude 74E 13" W; Fig. 1). It is comprised of >6 million acres of both privately owned land (3.3 million acres) and state protected Forest Preserve (2.7 million acres; APA 2001) and contains the entire range of the Adirondack Mountains. The ASP is mostly forested with a combination of northern hardwood and softwood stands scattered among numerous lakes and wetlands. The High Peaks area is mountainous with >40 peaks from 1,200 to >1,500 m elevation (Jenkins 2004). This area contains most of the original, old growth forests in the ASP as little harvesting or forest management occurred prior to the establishment of the ASP in 1984 (DiNunzio 1984).

The unique geographical characteristics and location with respect to Lake Ontario control most of the weather patterns, making it one of the coldest regions in the continental United States. The interior is usually 3 °C cooler than the bordering counties of upstate New York and Vermont; monthly winter temperatures range from −12 to −6 °C and summer temperatures range from 20–26 °C. The colder climate results in a short growing season (~180 days) with a mean of 85.8 mm of monthly precipitation (Garner 1989, Jenkins 2004). Topography and meteorological patterns influence the vegetation; southern species are more common along the periphery with cold-hardy species more plentiful in the boreal center

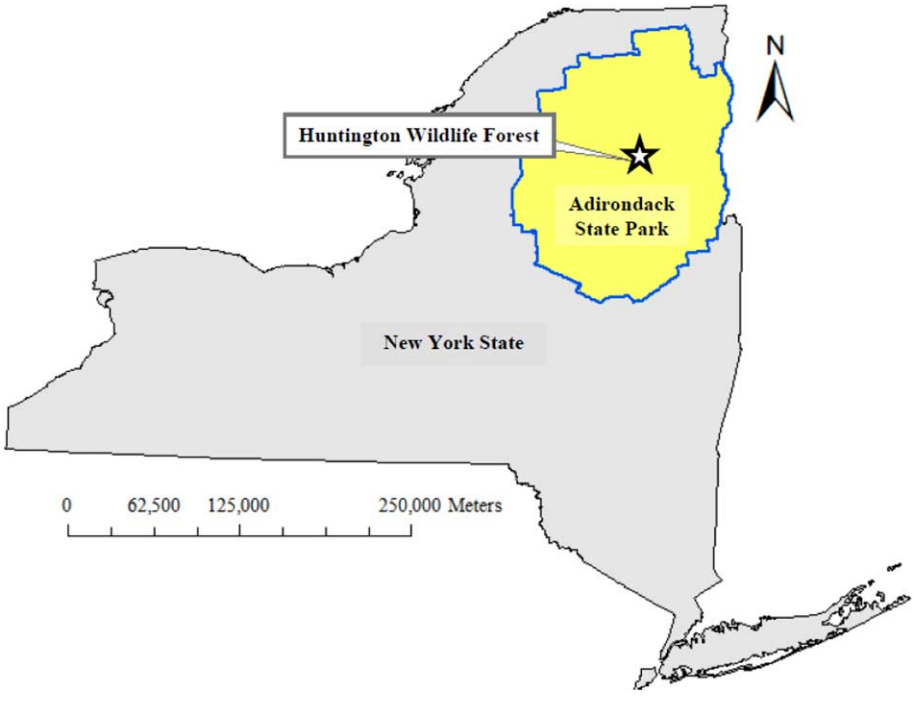

Fig. 1. Map of New York State, the Adirondack State Park, and Huntington Wildlife Forest.

(Jenkins 2004). Forestland in the ASP consists mostly of northern hardwoods including beech (*Fagus grandifolia*), red maple (*Acer rubrum*), sugar maple (*A. saccharum*), striped maple (*A. pensylvanicum*), and yellow birch (*Betula alleghaniensis*), and softwoods such as balsam fir (*Abies balsamea*), eastern hemlock (*Tsuga canadensis*), red spruce (*Picea rubens*), white cedar (*Thuja occidentalis*), and white pine (*Pinus strobus*). Shrubby vegetation, important for moose forage, includes witch hobble (*Viburnum alnifolium*), wild raisin (*V. cassinoides*), and other *Viburnum* species (Garner 1989).

METHODS

We used the United States Geological Survey's National Land Cover Datasets (NLCD 2001; resolution 30 m) obtained from the Adirondack Park Agency (APA) to quantify the necessary habitat characteristics of Model II in ArcGIS™ 9.3 (Table 1). All layers were clipped to the ASP boundary as it was our central focus for this study. Using Hawth's Tools (Beyer 2004) we overlaid a sampling grid on the ASP to designate 1028 evaluation units that reflected the approximate annual home range size of a moose, or about 25 km^2 (Allen et al. 1987, Koitzsch 2002, Hickey 2008). Regenerating habitat (V_1) and wetland habitat (V_2) were quantified using the methods of Hickey (2008) and evaluated against suitability figures developed for Model II approaches by Allen et al. (1987). Softwood (V_3) and old and mixed hardwoods (V_4) stands were designated as winter and summer cover, respectively. Because forest stand type can range in thermal cover characteristics, we condensed V_3 and V_4 into a single "thermal" cover variable (V_3) based on modeled operative temperature, and evaluated it against 2 suitability figures developed for the previous variables (Allen et al. 1987).

Table 1. Suitability classes, habitat variables and their optimal specifications (developed by Allen et al. 1987) for a new Habitat Suitability Index (HSI) model for moose in the Adirondack State Park, New York.

Suitability Class	Habitat Variables	Optimal Specification
Browse habitat	V_1: Hardwoods/mixed < 20 years	40% ≤ Area ≤ 50%
Aquatic habitat	V_2: Wetlands/open water	5% ≤ Area ≤ 10%
Thermal cover	V_3: Operative Temperature < UCT_e[1]	5% ≤ Area ≤ 55%

[1]Upper critical operative temperature (see text for details).

Thermal Cover (Habitat Variable V_3)

We separated the habitat analysis for thermal cover into 2 months (April and July) when moose are presumably susceptible to heat stress. In April moose are confronted with increasing daytime temperatures and insolation along with high surface albedo from accumulated snow, and in combination with molting winter pelage and increased metabolism, heat gain can be substantial (Renecker and Hudson 1986, 1990). Long days near maximal ambient temperature can also result in heat stress during July (Dussault et al. 2004).

To incorporate spatial variation associated with elevation, slope, and aspect, we used ArcGIS™ (ESRI 2010) to calculate mean monthly T_e for hardwood and softwood stands for each evaluation unit with the following equation (Campbell and Norman 1997):

$$T_e = T_a + \frac{r_e\left(R_{abs} - \varepsilon_s \sigma T_a^4\right)}{\rho c_p} \qquad (1)$$

where T_a is the ambient temperature (°C) evaluated at each unit, r_e is the animal's parallel resistance to convective and radiative heat transfer (s m^{-1}), R_{abs} is the total amount

of solar and thermal radiation absorbed by the animal (W m^{-2}), $\varepsilon_s \sigma T_a^4$ is the thermal emittance (W m^{-2}) of the surface of the animal (through tissue, skin, and pelage) at T_a (K), and ρc_p is the volumetric specific heat of air (1200 J m^{-3} per K; Table 2).

Table 2. Inputs to a model of operative temperature (T_e) for moose in the Adirondack State Park, New York.

Constant, Parameter or Variable	Source	Reference
Air temperature (T_a; C)	Modeled in ArcGIS	NCDC, CASTNET
Resistance to heat flow (r_e; sm^{-1})	$r_{Ha} \cdot r_r / r_{Ha} + r_r$	Beaver et al. 1996
Resistance to convective transfer (r_{Ha})	$307\sqrt{d/u} \cdot tf$	Campbell and Norman 1997
Characteristic dimension (d)	0.70 m^3	Mitchell 1976, Haase 2010
Average wind velocity (u)	1 ms^{-1}	Parker and Gillingham 1990
Turbulence factor (tf)	0.7	Campbell 1981
Resistance to long-wave transfer (r_r)	$\rho c_p / 4\varepsilon_s \sigma T_a^3$	Parker and Gillingham 1990
Emissivity of surface (ε_s)	0.97	Belovsky 1981
Stephan-Boltzmann constant (σ)	$5.67 \cdot 10^{-8}$ Wm^{-2} per K^4	Monteith 1973
Total radiation absorbed (R_{abs};/Wm^{-2})	SW + LW	Monteith 1973
Short-wave radiation	$a_s(A_p/A \cdot S_p + 0.5S_d + 0.5SWGR)$	Monteith 1973
Absorptivity to radiation (a_s)	0.74 summer, 0.89 winter	Belovsky 1981
View factor, or projected shadow area on a surface perpendicular to the beam (A_p/A) as a function of θ	$0.29-0.01(\theta/90)-0.31(\theta/90)^2+0.12(\theta/90)^3$	Kubaha et al. 2004; Haase 2010
Direct radiation corrected for the angle of incidence (S_p)	$S_b/\sin\theta$	Parker and Gillingham 1990
Diffuse short-wave radiation (S_d)	S_T * DiffFrac	Boland et al. 2001
Reflected short-wave radiation from the ground (SWGR)	Albedo · S_T	Parker and Gillingham 1990
Beam radiation incident on a horizontal surface (S_b)	S_T * BeamFrac	Boland et al. 2001
Total global radiation (S_T)	Modeled in ArcGIS™	ESRI 2010
Solar elevation angle (θ)	Dependent on Time of Day	Monteith 1973
Albedo	0.8 for snow, 0.2 for grass	Monteith and Unsworth 1990
Long-wave radiation (LW)	$a_L(0.5\varepsilon_{sky}\sigma T_a^4 + 0.5\varepsilon_{gr}\sigma T_a^4)$	Monteith 1973
Absorptivity to LW (a_L)	1.0 for caribou	Monteith 1973
Emissivity of sky (ε_{sky})	0.67 + 0.007*Ta in C	Gates 1980
Emissivity of the ground (ε_{gr})	0.97	Parker unpublished
Thermal emittance of the surface of the animal at T_a in K	$\varepsilon_s \sigma T_a^4$	Parker and Gillingham 1990
Volumetric specific heat of air	ρc_p	Monteith 1973

Ambient temperature (T_a) — We obtained air temperature data for April and July 2009 from 12 weather stations from the Environmental Protection Agency's Clean Air Status and Trend Network (CASTNET; http://www.epa.gove/castnet) and the National Climatic Data Center (NCDC; http://www.ncdc.noaa.gov) to model ambient temperature across the set of evaluation units. We used ordinary co-kriging of air temperature against a digital elevation model in ArcGIS™ to create a raster map with air temperature as a function of station elevation and separation distance. Geostatistical Analyst™ uses a take-one-out, cross-validation scheme for assessing goodness-of-fit of kriged surfaces. We used a three-step diagnostic process (Johnston et al. 2001, pp. 190–191) to validate modeled ambient temperatures, and then corrected them to 1 m above ground level using micro-meteorological stations established in the 2 forest canopy types (Haase 2010).

Resistance to total heat flow (r_e) — We calculated the thermal resistance to heat flow as a combination of the resistance to long-wave radiative heat transfer (r_r) and convective heat transfer (r_{Ha}). r_r was computed from the volumetric specific heat of air (ρc_p), the emissivity of the surface of the pelage (ε_s), the Stephan-Boltzman constant (σ), and ambient air temperature (T_a); r_{Ha} was calculated from the characteristic dimension (d) of a moose, the average wind velocity (u), and the turbulence factor (tf). All constants, parameters, and variables were initialized from the published literature except for characteristic dimension, wind velocity, and air temperature (Table 2). Because wind velocities below the forest canopy are usually low (DeMarchi 1991) and difficult to model, we used a constant wind velocity of 1m s^{-1} across all evaluation units (Parker and Gillingham 1990). Characteristic dimension was approximated as the volume of a sphere raised to the one-third power (Campbell and Norman 1998). We used data from Cameron et al. (1999: 96) and Hundertmark et al. (1997) to estimate mean volume to calculate the ratio of ingesta-free body mass to the density of water, muscle, fat, and bone of a 400 kg female moose (0.345 m^3).

Short- and long-wave radiation (R_{abs}) — Thermal radiation emitted from the surface of the animal ($\varepsilon_s \sigma T_a^4$) was calculated from the Stephan-Boltzmann constant in relation to air temperature and the emissivity of moose pelage (Table 2; Monteith 1973, Belovsky 1981). Total radiation (R_{abs}) was calculated as the sum of long- and short-wave radiation (Parker and Gillingham 1990). Long-wave radiation (LW) was calculated from emissivities of the ground and sky (dependent on air temperature) and absorptivities to long-wave heat transfer (Table 2; Beaver et al. 1996). Total short-wave radiation (SW) was calculated from modeled solar radiation in reference to seasonal resistances of the moose pelage to short-wave heat transfer (Table 2; Belovsky 1981, Parker and Gillingham 1990, Beaver et al. 1996).

The amount of solar radiation an animal is exposed to on the ground is a function of the amount of global radiation (direct and diffuse radiation) that is transmitted through the atmosphere, cloud cover, and forest canopy. Hourly global radiation was collected from a CASTNET weather station within the ASP on the Huntington Wildlife Forest (HWF187) and extraterrestrial radiation (i.e., above the atmosphere) was calculated based on the earth's distance from the sun in a model developed for the Solar Energy Research Institute (Bird and Hulstrom 1991). We calculated monthly averaged, hourly clearness indices (k_t, also referred to as cloudiness index), which is the ratio of global to extraterrestrial radiation for April and July (Haase 2010). We computed the mean monthly diffuse and beam fractions (Boland et al. 2001) with these

values by extrapolating average solar radiation at each intersection of a 100-m² grid using the Solar Analyst™ tool in ESRI's Spatial Analyst™. Finally, we kriged the point data to create raster maps representing monthly mean global, direct, and diffuse solar radiation at the top of the forest canopy for April and July.

We calculated the monthly fraction of solar radiation transmitted through the canopy associated with the 2 forest cover-types as:

$$\frac{G}{G_o} = BeamFrac(1 - SOF) + DiffFrac \bullet \overline{C}_o \quad (2)$$

where *BeamFrac* is the fraction of beam (i.e., direct) radiation through the atmosphere, *DiffFrac* is the fraction of diffuse radiation through the atmosphere, *SOF* is the sky obscuration factor of the canopy as a function of solar elevation zenith angle, and $\overline{C}_o$ is the total canopy opening factor for the canopy type (Lindroth and Perttu 1981).

We used hemispherical photography to calculate *SOF* and Gap Light Analyzer (GLA) software (version 2.0, Frazer et al. 1999) to calculate $\overline{C}_o$ (Hardy et al. 2004). We used a Nikon N2000 camera (integral-motor multi-mode 35 mm single-lens reflex) to take true color hemispherical photographs with a Sigma 8 mm F4 hemispherical lens (22.5 filter size) in April and July at 3 sites in each forest canopy cover-type (i.e., hardwood and softwood; 6 sites total) on Huntington Wildlife Forest. Each photograph was taken with the camera facing skyward, placed on a level tripod 1 m above the ground. The camera was positioned using a compass so the bottom faced south, allowing consistent registration of every photo. In GLA each photo was separated into "sky" or "non-sky" pixels using the image classification tools and overlaid with a sky map of grid cells to calculate canopy openness in each grid. Average transmission fractions were calculated for each forest cover-type and month (Lindroth and Perttu 1981). The NLCD 2001 raster was reclassified using the calculated transmission fractions for hardwood and softwood forest cover-types for each month. We averaged transmission fractions from both forest cover-types to represent the mixed forest cover-type; all other land-cover classes exhibited 100% radiation transmission (Lindroth and Perttu 1981). We multiplied the direct, diffuse, and global radiation raster maps by the canopy transmission fraction layer to produce new solar radiation layers with values adjusted for transmission through the forest canopy.

Classifying thermal cover — Schwab and Pitt (1991) adjusted the upper critical temperatures (UCT) measured by Renecker and Hudson (1986) onto T_e values of 0 °C in late winter and 20 °C in summer; likewise, they adjusted changes in respiration rate that resulted in panting for both late winter (UCT_e = 8 °C) and summer (UCT_e = 30 °C). Because thresholds were derived from moose acclimated to local conditions of Alberta, Canada, we re-scaled them proportionally to the prevailing difference in mean temperature regimes for the same period in the Adirondacks (Chaffee and Roberts 1971). The result was a respiration threshold increasing by 37.5% (i.e., UCT_e = 11 °C) for April and no change for July (i.e., UCT_e = 30 °C; data obtained by Weather Underground, www.wunderground.com). We computed T_e across all the evaluation units for both April and July and then re-classified the raster values as "thermally" suitable on the basis of T_e <UCT_e. Because moose use water bodies to dissipate heat, we reclassified areas with open water as thermal cover during July,

but assumed open water was inaccessible during April.

HSI Model II

Using figures developed by Allen et al. (1987), we designated suitability scores for each habitat variable within each evaluation unit. Scores were substituted into the HSI as:

$$\mathrm{HSI} = (V_1 * V_2 * V_3)^{1/3} \qquad (3)$$

HSI scores were projected in ArcGIS™ to show habitat suitability across the ASP and for each season. Evaluation units with scores <0.31 consisted of low habitat suitability, those with scores >0.67 were considered highly suitable (Koitzsch 2002, Hickey 2008), and those in between were considered moderately suitable. We computed the percentage of evaluation units in each suitability class to compare our classification to a published HSI model for the ASP that did not incorporate thermal cover (Hickey 2008).

In order to test that moose select suitable habitat designated by our model, we obtained moose observations (i.e., both visual and telemetry) from the New York State Department of Environmental Conservation (C. Dente, NYSDEC, pers. comm.) and the Adirondack Program of the Wildlife Conservation Society (M. Glennon, Wildlife Conservation Society, pers. comm.). We sorted the data by month and projected moose observations for April and July onto the appropriate seasonal suitability map. We performed a X^2 goodness-of-fit test on moose locations relative to the numbers expected in each suitability class based on area and compared standardized residuals among the 3 models (i.e., April, July, and Hickey 2008). No significant difference between expected and observed proportions indicated a correct classification relative to moose habitat use.

RESULTS

Mean monthly air temperatures derived from ordinary co-kriging ranged from 4.7–10.3 °C in April and 16.2–20.5 °C in July; prediction standard errors were relatively small (Fig. 2). Standardized root mean square errors (April: 0.88, July: 0.80) indicated that the model modestly overestimated variability in predicted temperatures. Forest canopy radiation transmission fractions varied by month and forest cover-type (Fig. 3), with the greatest decrease between April and July for hardwood stands (66.7 to 19.7% transmitted; P <0.0002). Softwood canopy transmission also declined (from 42.8 to 36.4%; P = 0.355), but not as dramatically. Average k_t values differed between months with April (k_t = 0.13) cloudier on average than July (k_t = 0.25; p-value = 0.031). Below-canopy solar radiation in April ranged from 69.0–212.2 Wm^{-2} and in July from 42.5–280.5 Wm^{-2}. T_e ranged from 5.6–15.3 °C during April (Fig. 4A), and from 19.0–29.1 °C during July (Fig. 4B). Thermal suitability increased from 59.9% of evaluation units below UCT_e in April, to 85.7% of evaluation units below UCT_e in July. The lowest T_e values corresponded closely to the highest elevations.

In April approximately 36.3% of evaluation units were characterized as low, 23.8% as moderate, and 39.7% as high suitability (Fig. 5A). Because average snow depth never exceeded 0.9 m, it was not included in our HSI (Schwab and Pitt 1991). During July the model classified 8.7% of the ASP as low, 16.6% as moderate, and 64.5% as high suitability (Fig. 5B). Highest suitability in both April and July occurred in a broad, crescent-shaped swathe extending from the north-central ASP westward and then south and eastward to the south-central ASP. Moderate to low suitability predominated in the eastern half of ASP.

There were 88 observations of moose in April in which 36.4% (n = 32) were located

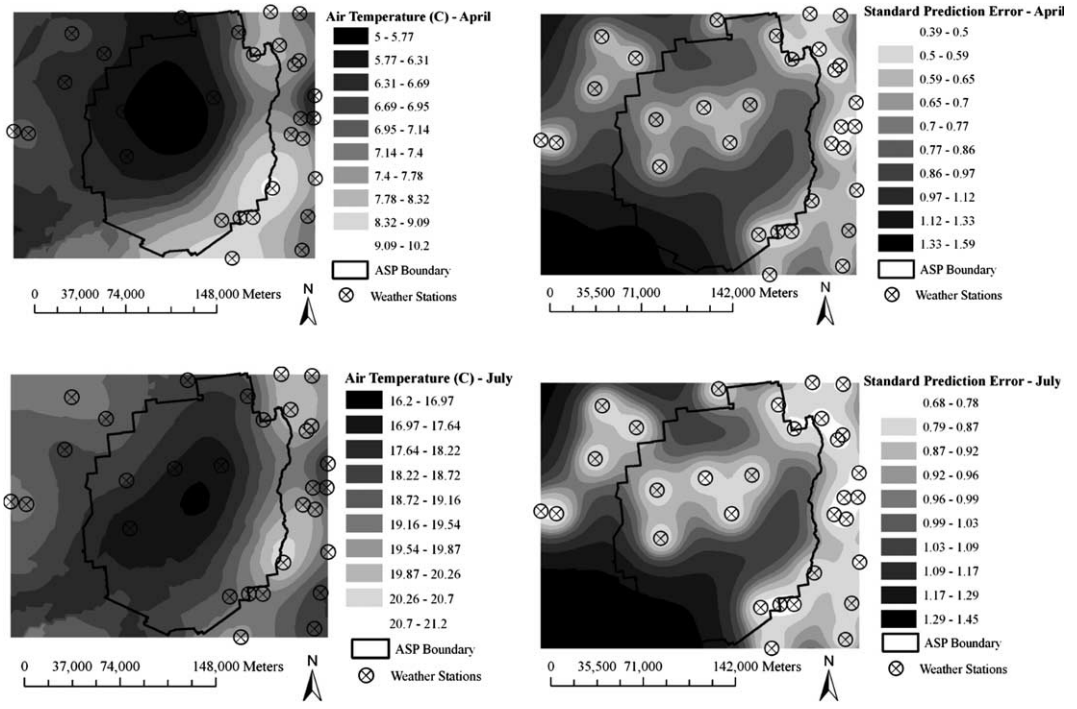

Fig. 2. Average air temperatures (C) for April and July and respective standard prediction error maps.

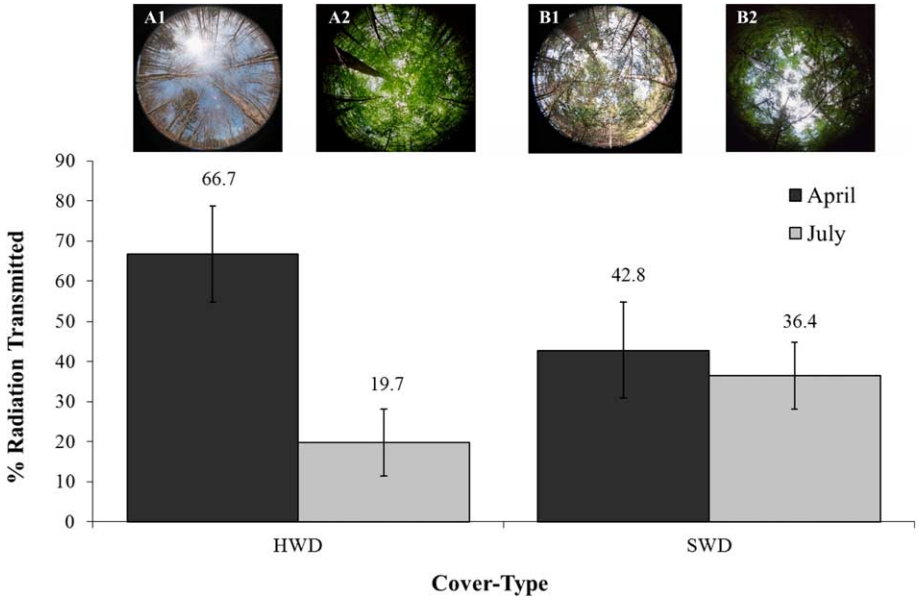

Fig. 3. Hemispherical photographs of (A) hardwood (HWD) and (B) softwood (SWD) stands in (1) April and (2) July on Huntington Wildlife Forest, New York and percent radiation transmission through respective forest canopy types (error bars represent one standard error).

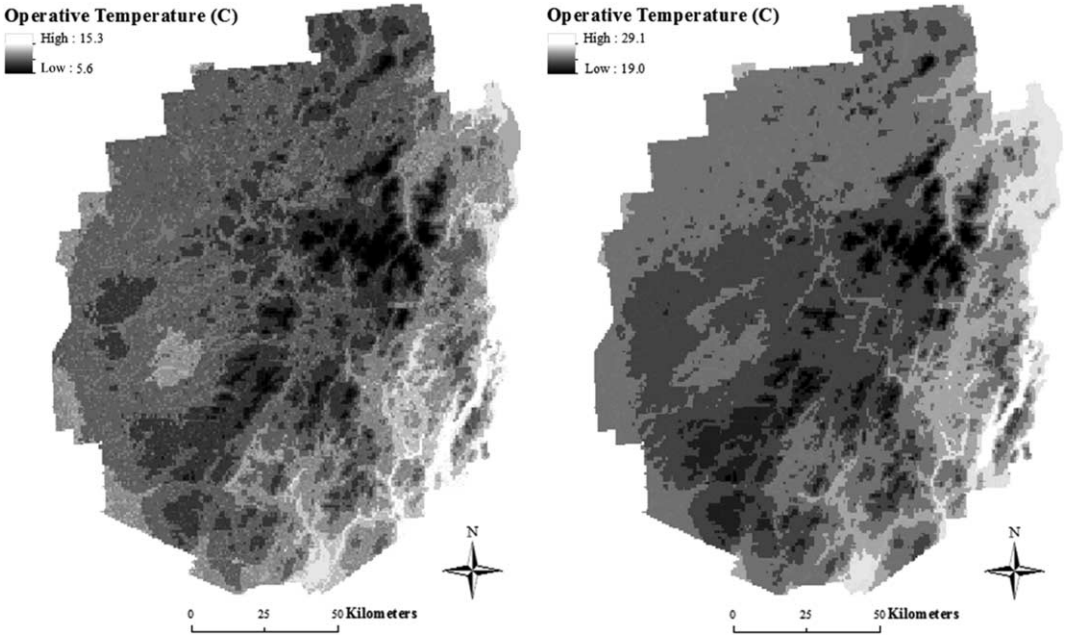

Fig. 4. Operative temperature (C) maps of the Adirondack State Park, New York for April (left) and July (right).

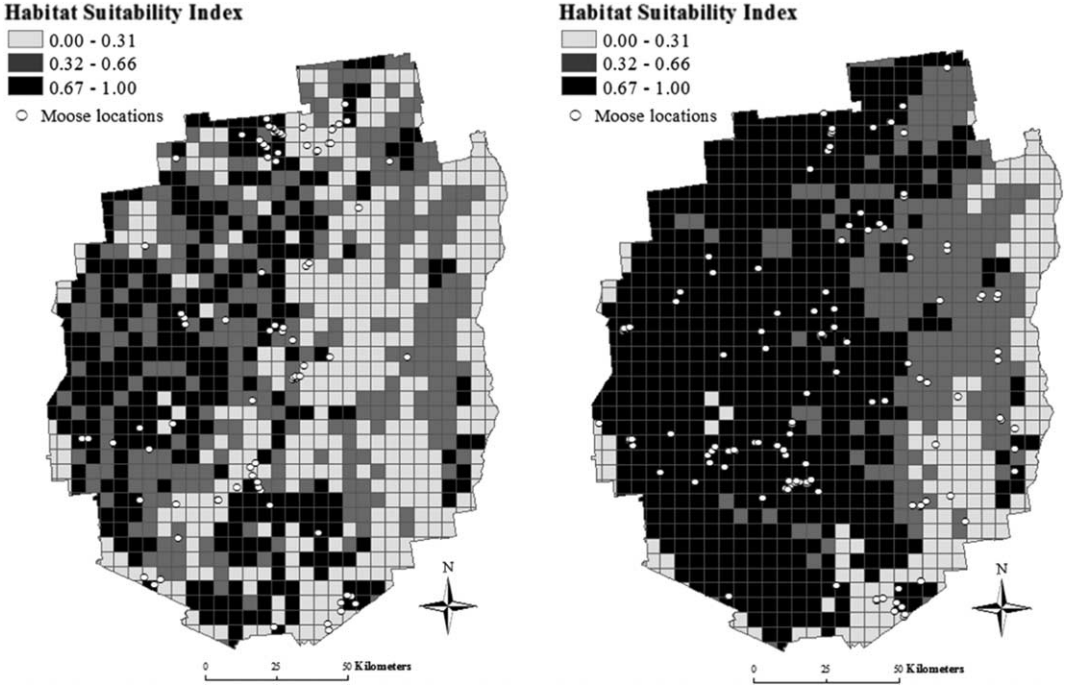

Fig. 5. April (left) and July (right) moose observations (white circles) on a modified habitat suitability map for the Adirondack State Park, New York.

in unsuitable, 23.9% (n = 21) in moderately suitable, and 39.8% (n = 35) in highly suitable habitat (Table 3, Fig. 5A). There were 150 moose observations in July, with 8.7% (n = 13) in unsuitable, 16.7% (n = 25) in moderately suitable, and 74.7% (n = 112) in highly suitable habitat (Table 3, Fig. 5B). The April model placed moose in suitability classes in proportion to expectation (X^2 = 4.5, P = 0.104, df = 2), whereas the July and Hickey (2008) models showed independence from the expected values (P <0.001, df = 2).

DISCUSSION

Habitat suitability modeling has been a mainstay of wildlife habitat management for over 30 years (Allen et al. 1987), and modern GIS technology has changed the use and application of HSI models. The use of remotely-sensed data has grown rapidly, while on-site, intensive habitat evaluation is becoming less common (Koitzsch 2002). In addition, complex mathematical operations on entire map layers can now be performed with relative ease (Fig. 4), and constructs like ESRI's ModelBuilder™ allows for a largely automated processing of data. Modeling represents the only practical way to explore spatial patterns of solar radiation, temperature, and physical elements affecting sunlight transmission through the forest canopy (DeMarchi and Bunnell 1995). Our approach combined modeling (i.e., parsing of the T_e equation), geospatial analysis (i.e., kriging of broad-scale spatial data), and field assessments of sub-canopy temperature and light regimes (i.e., hemispherical photography and micro-meteorology).

The statistical and computational methods for modeling geospatial data are well-documented (Johnston et al. 2001); for example, the digital elevation model was key to modeling solar radiation over complex topography (Fu and Rich 2002), and to co-kriging T_a to generate map layers as input to ModelBuilder™. Even with 12 stations, prediction standard errors for T_a were under 2 °C (Fig. 2), which we consider adequate for coarse evaluation of suitability. We acknowledge the limited scope of data used to estimate an average k_t for April and July, but because the majority of our weather results from synoptic-scale (≥1000 km) atmospheric disturbances (Bluestein 1992), we deemed the application of a measured k_t value at a single location as reasonable.

Hemispherical photography is widely used to characterize forest canopy structure (Frazer et al. 1999, Beaudet and Messier

Table 3. Number of observed (O) and expected (E) moose observations (1980–2000) in each suitability class by month, and the related X^2 statistic for a new HSI model developed for the Adirondack State Park, New York. Low suitability is an HSI score <0.31, moderate suitability is between 0.32 and 0.66, and high suitability is >0.67. Total number of evaluation units is 1028 and expected number of moose is proportional to area of each suitability class.

	April				July				Hickey (2008)			
Suitability Class	O	E	$(O-E)^2/E$	Std. Resid	O	E	$(O-E)^2/E$	Std. Resid	O	E	$(O-E)^2/E$	Std. Resid
Low	32	36	0.38	−0.62	13	30	9.56	−3.09	182	272	29.81	−5.46
Medium	21	26	1.00	−1.00	25	32	1.35	−1.16	1313	832	277.53	16.66
High	35	26	2.96	1.72	112	89	6.20	2.49	204	594	256.64	−16.02
X^2-statistic			4.5				17.1				564.0	
ASL[1]			0.104				<0.0001				<0.0001	

[1]Attained significance level, df = 2.

2002, Fu and Rich 2002, Hardy et al. 2004) and provides detailed characterization of the size and distribution of openings in the canopy, which we used to estimate radiation transmission fraction under forest cover-types (Fig. 3). While we replicated canopy measurements (n = 3 sites for each forest cover-type), we certainly did not capture sufficient range in variation of sub-canopy radiation transmission due to obscuration and stand management history. A much larger sampling effort would have been required; however, our transmission fractions fall within the range published for the northern hardwood forest (Domke et al. 2007; Fig. 3). Hardy et al. (2004) criticized the method we used to modify the above-canopy total irradiance, which neglects the roles of path lengths, sunflecks, tree geometry, and micro-topography on sub-canopy irradiance. We do not discount the criticism, but we believe the effects of those factors are less critical over the broad spatial scales we modeled.

The formulation of T_e we used is based on a model for mule deer (*Odocoileus hemionus*; Parker and Gillingham 1990) and domestic livestock (Beaver et al. 1996), and we made several modifications to fit our purpose (Table 2). First we modeled the diffuse fraction of solar radiation as a function of k_t and solar elevation angle (Boland et al. 2001). We also required a variable form for the view factor (Kubaha et al. 2004) to permit its calculation for any time of day (Haase 2010). In addition, rather than use a linear measurement as a surrogate for characteristic dimension, we computed it directly from volume by estimating carcass composition, body mass, and specific density of tissues (Mitchell 1976, Haase 2010). The more difficult challenge was mapping the respiratory threshold of Renecker and Hudson (1986) onto the T_e scale. Assuming that organisms become locally acclimated, it seemed reasonable to adjust their thresholds (Schwab and Pitt 1991) proportionally to the difference in average regional temperatures collected over the same time span, until thermoregulatory responses by moose in the Northeast are observed directly.

Developing a T_e model in ArcGIS™ allows for mapping of the thermal environment across the landscape. Despite the complexity of the calculations, crudeness of several data layers, and approximations to key determinants of T_e, our HSI model generates a more reasonable classification of moose habitat suitability than heretofore available (Table 3). Because we combined all 3 forest cover-types (i.e., hardwood, softwood, mixed) that were thermally suitable (i.e., $T_e < UCT_e$), our model classified fewer evaluation units in the high suitability class; therefore, the amount of thermal cover available for moose decreased as a consequence of the conflation. Assuming that few hardwood stands are thermally suitable in April, our HSI more accurately classified evaluation units as moderate and low suitability. Though the July model did a poorer job of correctly classifying moose observations, it improved upon the Hickey (2008) model that over-classified evaluation units into low and high suitability classes leaving the moderate habitat substantially under-classified (Table 3).

Due to the presence of industrial forest lands, it is generally accepted that the western half of the ASP has higher forage value for moose (Garner 1989). It also contained the largest area of highly suitable habitat based on our HSI, despite exhibiting mostly moderate thermal suitability (Fig. 5), indicating the complexity of evaluating the relative importance of forage and/or thermal cover to moose. The dramatic reduction in radiation transmitted through the forest canopy and the inclusion of open water boosted the suitability of eastern ASP during July; however, the 2 monthly maps differ mostly in extent, rather than location of highly suitable habitat.

Classifying habitat suitability by season is important, because aspects of the thermal environment and forage availability necessary for moose survival change throughout the year, particularly in the ASP (Fig. 5; Koitzsch 2002, Dussault et al.2006). Moose cope with thermal and nutritionally stressful environments and seasons through physiological and behavioral adaptations (Schwab and Pitt 1991, Dussault et al. 2004). Moose, in the short-term, cope with stressful thermal conditions by trading off time for space in favorable microhabitats (Bakken 1992, Parker and Gillingham 1990, Sargeant et al. 1994, Mysterud and Ostbye 1999). But, moose must maintain homeostasis in the long-term or face potentially deleterious individual and population consequences (Belovsky 1981, Dussault et al. 2004).

Our development of a moose HSI that incorporated thermal suitability agreed in general with known locations and suitable habitat of moose in the ASP. Along their southern range boundary moose are declining in certain areas (e.g., Minnesota, Lenarz et al. 2008) and appear to be thriving in others (e.g., Quebec, Ontario; Dussault et al. 2004, Lowe et al. 2010) despite ~5 ° difference in latitude. Habitat quality, forage abundance, effects of disease and parasites, density of white-tailed deer (see Lankester 2010), and combined effects of stress associated with warmer temperatures (see Murray et al. 2006, Lenarz et al. 2008) are possible explanations of regional and local differences in moose density and population response. Further elucidating the interrelationships of these factors, including the interaction of forage and thermal cover, is warranted to address a warming climate, differential population responses, and potential range shifts of moose.

ACKNOWLEDGEMENTS

We thank the members of the Quantitative Studies Laboratory and the Adirondack Ecological Center at the State University of New York College of Environmental Science and Forestry and Dr. M. Glennon of the Wildlife Conservation Society for field and technical support. We thank 2 anonymous reviewers for substantially improving an earlier draft of this manuscript. Funding was provided by the Edna B. Sussman Foundation and the Sigma Xi Research Society.

REFERENCES

Adirondack Park Agency (APA). 2001. State of New York Adirondack Park State Master Plan. Ray Brook, New York, USA.

Allen, A.W., P. A. Jordan, and J. W. Terrell. 1987. Habitat suitability index models: moose, Lake Superior region. United States Fish and Wildlife Service Biological Report 82 (10.155), Fort Collins, Colorado, USA.

Bakken, G. S. 1992. Measurement and application of operative and standard operative temperatures in ecology. American Zoology 32: 194–216.

Beaudet, M., and C. Messier. 2002. Variation in canopy openness and light transmission following selection cutting in northern hardwood stands: an assessment based on hemispherical photographs. Agricultural and Forest Meteorology 110: 217–228.

Beaver, J. M., B. E. Olson, and J. M. Wraith. 1996. A simple index of standard operative temperature for mule deer and cattle in winter. Journal of Thermal Biology 21: 345–352.

Belovsky, G. E. 1981. Optimal activity times and habitat choices of moose. Oecologica 48: 22–30.

Beyer, H. L. 2004. Hawth's Analysis Tools for ArcGIS. <http://www.spatialecology.com/htools> (accessed 2010).

Bird, R. E., and R. L Hulstrom. 1991. A simplified clear sky model for direct and diffuse insolation on horizontal s urfaces. SERI Technical Report SERI/

TR-642–761. Energy Research Institute, Golden, Colorado, USA.

BLUESTEIN, H. B. 1992. Synoptic-Dynamic Meteorology in Midlatitudes: Principles of Kinematics and Dynamics. Vol. 1. Oxford University Press, Oxford, England.

BOLAND, J., L. SCOTT, and M. LUTHER. 2001. Modeling the diffuse fraction of global solar radiation on a horizontal surface. Environmetrics 12: 103–116.

CAMERON, J. R., J. G. SKOFRONICK, and R. M. GRANT. 1999. Physics of the Body. Second Edition. Medical Physics Publishing, Madison, Wisconsin, USA.

CAMPBELL, G. S. 1981. Fundamentals of radiation and temperature relations. Pages 11–40 *in* O. L. Lange, P. S. Nobel, C. B. Osmond, and H. Ziegler, editors. Encyclopedia of Plant Pathology. Vol. 12A, Physiological Plant Ecology I. Springer-Verlag, Berlin, Germany.

———, and J. M. NORMAN. 1997. An Introduction to Environmental Biophysics, 2nd Edition. Springer, New York, New York, USA.

CHAFFEE, R. R., and J. C. ROBERTS. 1971. Temperature acclimation in birds and mammals. Annual Review of Physiology 33: 155–202.

DEMARCHI, M. W. 1991. Influence of the thermal environment on forest cover selection and activity of moose in summer. M. S. Thesis, University of British Columbia, Vancouver, British Columbia, Canada.

———, and F. L. BUNNELL. 1995. Forest cover selection and activity of cow moose in summer. Acta Theriologica 40: 23–36.

DETTKI, H., R. LÖFSTRAND, and L. EDENIUS. 2003. Modeling habitat suitability for moose in coastal northern Sweden: empirical vs. process-oriented approaches. Ambio 32: 549–56.

DINUNZIO, M. G. 1984. Adirondack Wildguide. Adirondack Conservancy Committee and Adirondack Council, Elizabethtown, New York, USA.

DOMKE, G. M., J. P. CASPERSEN, and T. A. JONES. 2007. Light attenuation following selection harvesting in northern hardwood forests. Forest Ecology and Management 239: 182–190.

DUSSAULT, C., R. COURTOIS, and J. J. -P. OUELLET. 2006. A habitat suitability index model to assess moose habitat selection at multiple spatial scales. Canadian Journal of Forest Resources 36: 1097–1107.

———, J. -P. OUELLET, R. COURTOIS, J. HUOT, L. BRETON, and J. LAROCHELLE. 2004. Behavioral responses of moose to thermal conditions in the boreal forest. Ecoscience 11: 321–328.

FRAZER, G. W., C. D. CANHAM, and K. P. LERTZMAN. 1999. Gap Light Analyzer (GLA), Version 2.0: Imaging software to extract canopy structure and gap light transmission indices from true-colour fisheye photographs, user's manual and program documentation. Simon Fraser University, Burnbay, British Columbia, Canada and the Institute of Ecosystem Studies, Millbrook, New York, USA.

FU, P., and P. M. RICH. 2002. A geometric solar radiation model with applications in agriculture and forestry. Computers and Electronics in Agriculture 37: 25–35.

GARNER, D. L. 1989. Ecology of the moose and the feasibility for translocation into the Greater Adirondack Ecosystem. M. S. Thesis, SUNY College of Environmental Science and Forestry, Syracuse, New York, USA.

GATES, D. M. 1980. Biophysical Ecology. Springer-Verlag, New York, New York, USA..

GUISAN, A., and N. E. ZIMMERMANN. 2000. Predictive habitat distribution models in ecology. Ecological Modeling 135: 147–186.

HAASE, C. G. 2010. Characterizing critical thermal environments for moose (*Alces alces*) in the Adirondack Mountains of New York. M. S. Thesis, SUNY College

of Environmental Science & Forestry, Syracuse, New York, USA.

HARDY, J. P., P. MELLOH, G. KOENIN, D. MARKS, A. WINSTRAL, J. W. POMEROY, and T. LINK. 2004. Solar radiation transmission through conifer canopies. Agricultural and Forest Meteorology 126: 257–270.

HICKEY, L. 2008. Assessing the recolonization of moose in New York with HSI models. Alces 44: 117–126.

HUNDERTMARK, K. J., C. C. SCHWARTZ, and T. R. STEPHENSON. 1997. Estimation of body composition in moose. Federal Aid in Wildlife Restoration Final Report. Alaska Department of Fish and Game, Division of Wildlife Conservation, Juneau, Alaska, USA.

JENKINS, J. 2004. The Adirondack Atlas: A Geographic Portrait of the Adirondack Park. Wildlife Conservation Society, Bronx, New York, USA.

JOHNSTON, K., J. M. VER HOEF, K. KRIVORUCHKO, and N. LUCAS. 2001. Using ArcGIS™ Geostatistical Analyst™. ESRI, Redlands, California, USA <http://www.esri.com> (accessed 2010).

KOITZSCH, K. B. 2002. Application of a moose habitat suitability index model to Vermont wildlife. Alces 38: 89–107.

KUBAHA, K., D. FIALA, J. TOFTUM, and A. H. TAKI. 2004. Human projected area factor for detailed direct and diffuse solar radiation analysis. International Journal of Biometeorology 49: 113–129.

LANKESTER, M. W. 2010. Understanding the impact of meningeal worm, *Parelaphostrongylus tenuis*, on moose populations. Alces 46: 53–70.

LENARZ, M., M. E. NELSON, M. W. SCHRAGE, and A. J. EDWARDS. 2008. Temperature mediated moose survival in northeastern Minnesota. Journal of Wildlife Management 73: 503–511.

LINDROTH, A., and K. PERTTU. 1981. Simple calculation of extinction coefficient of forest stands. Agricultural Meteorology 25: 97–110.

LOWE, S. J., B. R. PATTERSON, and J. A. SCHAEFER. 2010. Lack of behavioral responses of moose (*Alces alces*) to high ambient temperatures near the southern periphery of their range. Canadian Journal of Zoology 88: 1032–1041.

MITCHELL, J. W. 1976. Heat transfer from spheres and other animals. Biophysical Journal 16: 561–569.

MOEN, A. N. 1968. Critical thermal environment: a new look at an old concept. Bioscience 18: 1041–1043.

MONTEITH, J. L. 1973. Principles of Environmental Physics. American Elsevier, New York, New York, USA.

———, and M. H. UNSWORTH. 1990. Principles of Environmental Physics. Second Edition. Edward Arnold, New York, New York, USA.

MURRAY, D. L., E. W. COX, W. B. BALLARD, H. A. WHITLAW, M. S. LENARZ, T. W. CUSTER, T. BARNETT, and T. K. FULLER. 2006. Pathogens, nutritional deficiency, and climate influences on a declining moose population. Wildlife Monographs 166: 1–30.

MYSTERUD, A., and E. OSTBYE. 1999. Cover as a habitat element for temperate ungulates: effects on habitat selection and demography. Wildlife Society Bulletin 27: 385–394.

PARKER, K. L., and M. P. GILLINGHAM. 1990. Estimates of critical thermal environments for mule deer. Journal of Range Management 43: 73–81.

PUTTOCK, G. D., P. SHAKOTKO, and J. G. RASAPUTRA. 1995. An empirical habitat model for moose, *Alces alces*, in Algonquin Park, Ontario. Forest Ecology and Management 81: 169–178.

RENECKER, L. A., and R. J. HUDSON. 1986. Seasonal energy expenditures and thermoregulatory response of moose. Canadian Journal of Zoology 64: 322–27.

———, and ———. 1990. Behavioral and thermoregulatory responses of moose to high ambient temperatures and insect

harassment in aspen dominated forests. Alces 26: 66–72.

ROMITO, T., K. SMITH, B. BECK, J. BECK, M. TODD, R. BONAR, and R. QUINLAN. 1999. Moose winter habitat suitability index model. Version 5. Foothills Model Forest, Alberta, Canada.

SARGEANT, G. A., L. E. EBERHARDT, and J. M. PEEK. 1994. Thermoregulation by mule deer (*Odocoileus hemionus*) in arid rangelands of southcentral Washington. Journal of Mammalogy 75: 536–544.

SCHWAB, F. E., and M. D. PITT. 1991. Moose selection of canopy cover types related to operative temperature, forage, and snow depth. Canadian Journal of Zoology 69: 3071–3077.